Journal of Neuroscience Methods

A low-cost telescope for enhanced stimulus visual field coverage in functional MRI

--Manuscript Draft--

Manuscript Number:	JNEUMETH-D-20-00439R1
Article Type:	Research Paper
Section/Category:	Clinical Neuroscience
Keywords:	telescope; visual field; fMRI; visual cortex
Corresponding Author:	Jasleen Kaur Jolly, DPhil University of Oxford Oxford, UNITED KINGDOM
First Author:	Jasleen Kaur Jolly, DPhil
Order of Authors:	Jasleen Kaur Jolly, DPhil
	Aislin A Sheldon
	Ivan Alvarez
	Chris Gallagher
	Robert E MacLaren
	Holly Bridge
Abstract:	Background A common limitation of typical projection systems used for visual fMRI is the limited field of view that can be presented to the observer within the scanner. A wide field of view over which stimuli can be presented is critical when investigating peripheral visual function, in particular visual disorders or diseases that lead to the loss of peripheral vision. New method We present a relatively low-cost Galilean telescopic device that can be used in most MRI scanners to double the effective visual field being presented. The system described is non-ferromagnetic, and compatible with most standard methods of visual presentation in MRI environments. The increase in area of visual cortex activation was quantified by comparing the extent of visual activity evoked by observing flickering checkerboards with and without the telescope in place. Results In all three observers that reported image fusion from the telescope, the extent of cortical activation was greater with the telescope, while in the fourth observer there was no difference between the two methods due to a lack of fusion. Conclusion The telescope is a low cost, easy to implement solution in situations where changes to the existing equipment or setup are not feasible.
Response to Reviewers:	

Powered by Editorial Manager® and ProduXion Manager® from Aries Systems Corporation

Ethical Standards Agreement

Click here to access/download;Ethical Standards Agreement;ethical_standards_agreement.doc

We have read and have abided by the statement of ethical standards for manuscripts submitted to the Journal of Neuroscience Methods.

ETHICAL STANDARDS:

- The authors declare that all experiments on human subjects were conducted in accordance with the Declaration of Helsinki http://www.wma.net and that all procedures were carried out with the adequate understanding and written consent of the subjects.

- The authors also certify that formal approval to conduct the experiments described has been obtained from the human subjects review board of their institution and could be provided upon request.

- The authors also certify that formal approval to conduct the experiments described has been obtained from the animal subjects review board of their institution and could be provided upon request.

- The Editors reserve the right to return manuscripts in which there is any question as to the appropriate and ethical use of human or animal subjects.

NUFFIELD DEPARTMENT OF CLINICAL NEUROSCIENCES
UNIVERSITY OF OXFORD
Dr Jasleen Kaur Jolly DPhil MSc MCOptom
Level 6, West Wing, John Radcliffe Hospital, Oxford OX3 9DU
Email: jasleen.jolly@eye.ox.ac.uk Web: www.eye.ox.ac.uk

22nd October 2020

Dear Prof Di Giovanni,
Thank you for the helpful comments and the opportunity to revise the manuscript. Please find enclosed a point by point response.

Reviewer: 1
Dear Editor and Authors,
I think that authors very well answered the previous reviewer comments. I recommend the publication of this paper offering a convincing presentation (and validation) of an original system for fMRI visual stimulation. I suggest below some minor improvements.
For me, this sentence "foveal spatial frequencies spanning 4.35 cpd at the fovea and 1.18 cpd at the most eccentric point" is very unclear. Maybe an explanation for no specialist reader would be welcomed.

Thank you for the encouragement. This sentence on page 8, line 147 has now been changed to, "The spatial frequencies increased from the centre to the periphery, using a base 10 log function, to account for eccentricity scaling within the visual cortex. The spatial frequency measured 4.35 cycles per degree (cpd) at the fovea and 1.18 cpd at the most eccentric point."

The sentence "an increase in the volume of activated tissue using the telescope, evident both in the flattened, and volume view." Could be favorably replaced or completed by the size (in pixels) of the activations.

We have added in analysis of the number of voxels activated as Table 1 on page 11. This has been added into the text on page 10 line 207, "This increase in activation is represented by the number of voxels activated in the primary visual cortex (V1) shown in Table 1."

Regarding the first level results presentation, I do not agree the current choice: a volume presentation for the large stimulus and a flat one for the medium and small stimulus. Authors have to choose one kind of presentation (may be flat to be in accordance with fig. 6) for the three different stimuli. Again, a table with the activation sizes for the three stimuli, with and without telescope would be an improvement.

Clearly there is a difference in opinion relating to the preferred method of visualisation. We realise there is redundancy in showing both the flat and volume views however, we hope that this means the data are interpretable by all readers. Thank you for the helpful comment on activation size, we have added a table showing this on page 11.

On both figures 4 and 5, "telescope" activation is presented with a color scale as "no telescope" activation is presented with a solid color. Why this difference?

Thank you for pointing this out, this has been corrected, so now so they all show a solid colour.

Reviewer: 2

This manuscript by Jolly JK et al. describes a low cost Galilean optics-based telescope designed for visual stimulation for fMRI. The objectives are straightforward and the methods and results described

seem to achieve the objectives. This study may allow fabrication of similar equipment by other investigators who may not have access to expensive company-built devises. Although it looks like an original submission, I also saw comments by another reviewer, and responses and text changes thereof. They give the impression that in this probable resubmission the authors have revised the text and increased the quality of the submission. However, it could be further strengthened by including details of lens preparation that is crucial for others to replicate the methods.

Major
1. Does preparation of the lenses described in the study require access to an optical machine shop to grinding the lenses to the needed specification? Or can they be outsourced?

Our lenses were cut within the local workshop. Any machine able to lathe plastic lenses will be able to meet the specifications. The size details are in the CAD design files. This point has been added into methods section, page 4 line 79, "They can be cut to size by any lab containing a lathe compatible with plastic lenses."

Minor
1. There are some typos (e.g., 'cortical activation measurable' in Highlights)

This has been altered to, "This results in an increase in cortical activation that is measurable."

Reviewer: 3
Major comments:
The authors developed a low-cost telescope to increase the field of view (FOV) of visual stimulation in the MRI scanner. The maximum FOV demonstrated in this study is only 29 degrees in diameter. Since one of the goals of increasing FOV is to map the cortical representations of peripheral vision in healthy participants or patients, 29-degree FOV is not a major advancement compared with what has already been achieved in the field of visual mapping.

Thank you for your comments. We appreciate the increase in FOV is not large. However, standard perimetry techniques such as Humphrey fields or microperimetry routinely measure the central 30 degrees. By extending the FOV to match this we allow the fMRI data and visual field data to be correlated directly. This point has been added to the discussion on page 14 line 269, "By expanding the field of view to a similar level, we allow the results from fMRI to be directly correlated with visual field testing due to the same area being covered."

It is actually not that difficult to set up a wide-field (100-deg) projection screen in the MRI scanner, as demonstrated by Pitalis, Sereno, Huang, and other groups. The authors cited Sereno et al., 1995 as well as Pitalis et al., 2013, indicating they are aware of the advancement in the field of visual mapping Furthermore, Wada et al. (Frontiers in Psychology, 2016) were able to present visual stimuli with 100-deg FOV using telescopes and activated high-level motion areas containing mostly peripheral representations.

We agree that these other mechanisms would be best practice. However, our scanners are shared by multiple research groups so the permission to install this system was not granted. Additionally the system proposed costs hundreds of pounds rather than thousands of pounds for the other systems available. We therefore feel it has a place. Particularly in cases when relating to clinical data as detailed above.

The benchmark of a wide-field visual mapping study is to activate areas V6, V6A, MT/MST, CSv, VIP, precuneus, and PIC. However, visual activations shown in this study were strictly limited to early visual areas (V1-V4).
For clinical applications, visual stimulation with a 30-deg FOV (15-deg eccentricity) is insufficient to detect and map the loss of peripheral vision.

Together, this study did not demonstrate sufficient technical and scientific advancement to justify its publication in the Journal of Neuroscience Methods.

In many retinal disease there is significant degeneration of the retina and therefore the visual input within the central 30 degrees and this would be picked up with the telescope system. This was our motivation in developing this system. You are correct that it would not be suitable for true periphery or for studies with different outcomes.

Minor comments:
The telescope is only tested with the 64-channel coil in a Siemens Prisma 3T MRI scanner. It is not clear whether the telescope system could be readily used for other head coils (e.g., 32 channel coil) in Siemens Prisma or other scanner/coil models of Siemens or GE.

Thank you for highlighting this. The materials used will not be incompatible with any other MRI setups. The limiting factor will be the distances available to fit the telescope into. This has been highlighted in the discussion, page 14 line 288, "For other scanners and head coils the system can be adapted by adjusting the lens powers and distances used."

Many thanks to the editors and reviewers for the guidance and comments.

Many kind regards,

Dr Jasleen K Jolly, DPhil MSc MCOptom
Senior Clinical Research Fellow

Aislin Sheldon MSc
DPhil Candidate

Prof Holly Bridge DPhil FRS
Professor of Neuroscience

*Title page-incl. type of article and authors name and affiliation Click here to access/download;Title page-incl. type of article and authors name and affiliation;Title page.docx

A low-cost telescope for enhanced stimulus visual field coverage in functional MRI.

Jasleen K. Jolly DPhil MCOptom[1-3* #], Aislin A. Sheldon MPsych[1,3 #], Ivan Alvarez PhD[1,3], Chris Gallagher BSc[3], Robert E. MacLaren DPhil FRCOphth[1-2], Holly Bridge DPhil[1,3]

[1]Nuffield Department of Clinical Neurosciences, University of Oxford, Oxford, United Kingdom
[2]Oxford Eye Hospital, Oxford University Hospitals NHS Foundation Trust, Oxford, United Kingdom
[3]Oxford Centre for Functional MRI of the Brain (FMRIB), Wellcome Centre for Integrative Neuroimaging, University of Oxford, Oxford, OX3 9DU, UK

# Equal contribution to this work.

* Corresponding author. Centre for Functional Magnetic Resonance Imaging of the Brain, Nuffield Department of Clinical Neurosciences, John Radcliffe Hospital, Headley Way, Headington, Oxford OX3 9DU. Email address: jasleen.jolly@ndcn.ox.ac.uk

Financial: This article presents independent research funded by the National Institute for Health Research (NIHR) [Clinical Doctoral Research Fellowship CA-CDRF-2016-02-002 for Jasleen K Jolly], the Medical Research Council (MR/K014382/1) and The Royal Society (University Research Fellowship to HB). The Wellcome Centre for Integrative Neuroimaging is supported by core funding from the Wellcome Trust (203139/Z/16/Z). The views expressed are those of the authors and not necessarily those of the NHS, the NIHR or the Department of Health. The sponsor and funding organization had no role in the design or conduct of this research.

Research article

Highlights

- A low costs MR safe device can be constructed to expand the amount of visual field being examined in the scanner.
- This can be attached to existing head coils.
- It works well when refractive error is fully corrected and participant can maintain binocular fusion. This results in an increase in cortical activation that is measurable.

Manuscript with changes marked

Click here to access/download;Manuscript (With Page Numbers);Telescope paper

Abstract

Background

A common limitation of typical projection systems used for visual fMRI is the limited field of view that can be presented to the observer within the scanner. A wide field of view over which stimuli can be presented is critical when investigating peripheral visual function, in particular visual disorders or diseases that lead to the loss of peripheral vision.

New method

We present a relatively low-cost Galilean telescopic device that can be used in most MRI scanners to double the effective visual field being presented. The system described is non-ferromagnetic, and compatible with most standard methods of visual presentation in MRI environments. The increase in area of visual cortex activation was quantified by comparing the extent of visual activity evoked by observing flickering checkerboards with and without the telescope in place.

Results

In all three observers that reported image fusion from the telescope, the extent of cortical activation was greater with the telescope, while in the fourth observer there was no difference between the two methods due to a lack of fusion.

Conclusion

The telescope is a low cost, easy to implement solution in situations where changes to the existing equipment or setup are not feasible.

Keywords: telescope; visual field; fMRI; visual cortex

Introduction

The early visual system is mapped in retinotopic coordinates, such that points that are adjacent to each other in the visual scene are represented by neighbouring neurons. This is the case from the photoreceptor cells in the retina through to the cerebral cortex, and provides the theoretical basis for retinotopic mapping; the identification of visual areas based on having one whole representation of visual space (Bridge, 2011; DeYoe et al., 1996; Sereno et al., 1995; Tootell et al., 1998).

Functional magnetic resonance imaging (fMRI) studies exploit retinotopy to identify different visual areas noninvasively. However, while the visual field of view is around 150° in natural vision, the limited space within the MRI environment significantly reduces the region visible from inside the scanner bore. Although the central visual field has considerably greater neural representation, known as cortical magnification (Wandell et al., 2007), there are many situations when peripheral stimulation is important (DeYoe et al., 2015). Firstly, in retinotopic mapping, the greater the stimulated region, the larger area of visual representation mapped in the cortex (Tootell et al., 1998). Secondly, some extrastriate visual areas, such as V6 and V6A primarily contain representations of the peripheral visual field, and cannot be accurately localised without far peripheral stimulation (Pitzalis et al., 2013). Thirdly, a lack of peripheral stimulation is a particular challenge when mapping the visual field in participants with eye disease that affects the periphery such as glaucoma, and rod-cone dystrophies (Brown et al., 2016; Silson et al., 2018). In the early stages of these conditions, vision loss can begin outside the area measurable by standard presentation methods. Therefore the cortical representation of this vision loss is not measured until the late stages of disease progression (Brown et al., 2016; Dumoulin and Knapen, 2018).

A number of different approaches are used to provide visual stimulation within the scanner environment, with one of the most common being a digital display placed at the end of the scanner bore. The screen is typically viewed using a standard mirror placed above the head of the scan participant, who lies supine on the scanner bed. This setup is limited by physical constraints, such as the scanner bore size, distance between the mirror and screen, and the physical apertures for the eyes provided in the head coil. A head-mounted goggle system can provide larger visual field coverage by using screens close to the eye (8,9). The main drawback of this type of system is the cost, which is significantly greater than other

presentation systems, and may not be suitable for participants with larger head sizes due to the space in the head coil. Another approach used to increase the stimulated field of view is a projector system with a target screen set close to the participant inside the scanner bore (Roby et al., 2000), but constraints on space make this option impossible for some scanning environments. Furthermore, errors can be induced by the close proximity of the screen to the eyes inducing convergence or accommodative errors. Solutions that require permanent installation of equipment are not feasible in scanner sites shared between multiple teams. The options available for presenting stimuli dichoptically have been previously comprehensively reviewed (Choubey et al., 2009), and include a system relying on Keplerian binoculars to separate the images to the two eyes (Neri et al., 2004).

In visual stimulation experiments using a screen outside the scanner bore, the stimulus typically extends up to around 13 degrees radius, though this varies on the specific setup in any particular center (Dumoulin and Wandell, 2008), with some set-ups reaching a maximum field of view with a radius up to 15 degrees (Baseler et al., 2011). Using a wide projection screen viewed directly without a mirror can increase the visual field up to 100 degrees (Pitzalis et al., 2013). However, this type of wide projection screen is difficult to set up due to the space requirements.

Telescopic systems allow the magnification of the stimulus, and therefore a greater area of the visual field to be covered by the stimulus. They can be attached directly to a standard MRI mirror, thus keeping the cost of the system low, and the time to implement short. Telescopes consist of two lenses set at specific distances from the eye and from each other in order to achieve optical magnification of the image. There are two telescopic designs that allow the creation of an image that is both magnified, and correctly oriented. Keplerian (or astronomical) telescopes as implemented in binoculars used previously (Backus et al., 2001; Neri et al., 2004) allow for greater levels of magnification but are generally large, and create an inverted image that must be rectified (albeit rectified by commercial binoculars). Nonetheless, the binoculars used previously relied on use of a surface coil on the occipital lobe, rather than the modern 64-channel head coils. Galilean telescopes are shorter and create a non-inverted image, therefore allowing for a more compact construction that is able to fit into the space available in the MRI environment between the eye and the head coil (Dickinson, 2002). The latter design was therefore chosen to fit in the limited space available

(Figure 1). The Galilean design is used in low vision devices such as the Eschenbach Max range which forms the inspiration for the design proposed.

Materials and Methods

Galilean telescope-based device

The principles of the design are shown in Figure 1. In our particular implementation, the objective lens had a power of +16.7D and the eyepiece lens had a power of -33D (Figure 2A and B). The lenses were placed 3cm apart so their focal lengths coincided, and the system was placed 3cm from the eye (Figure 2C). This resulted in 2x magnification as calculated by $M = -F_e / F_o$ (Figure 2D and E). In our test case using a 64-channel head coil (Siemens Healthcare, Erlangen, Germany) for a 3T Prisma MRI (Siemens Healthcare, Erlangen, Germany), the maximum space available between the MR safe glasses to the rim of the head coil was 3.6cm for both refractive correction and the telescopic system. This was a constraining factor for the lens powers that could be used. We also wanted to keep the objective lens as large as possible to maximise the field of view as the exit pupil diameter is equal to the objective lens diameter divided by the magnification. The lenses were crafted in polymethyl methacrylate with a refractive index of 1.4906 and no additional coating. They can be cut to size by any lab containing a lathe compatible with plastic lenses.

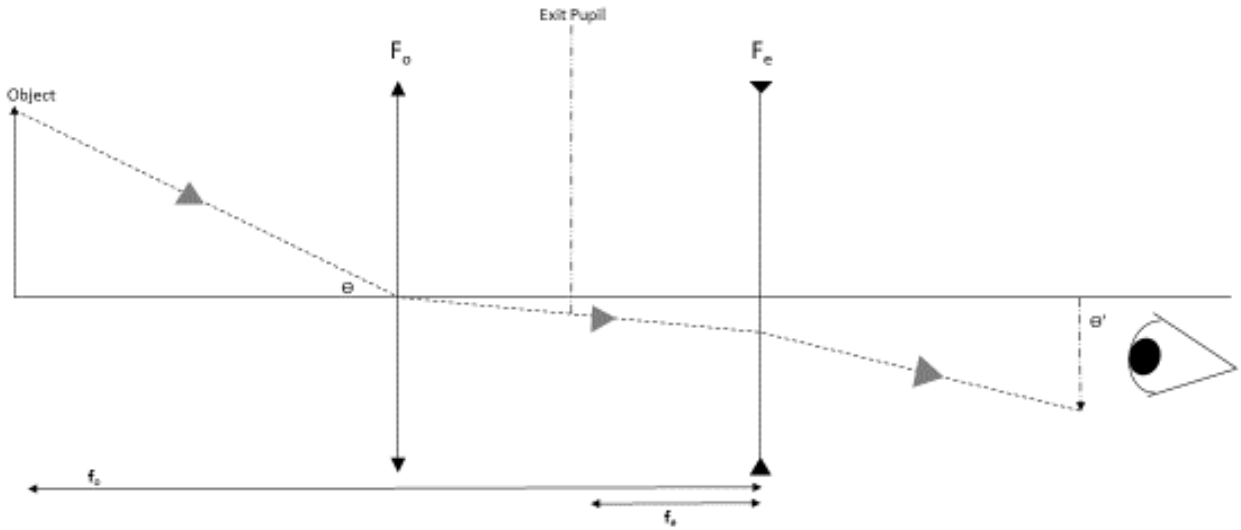

Figure 1: Ray diagram showing the principles of the Galilean telescope. The object extends angle Θ at the positive objective lens (F_o) and the image subtends angle Θ` at the eye. F_e denotes the negative eyepiece lens. The dotted line shows the path of light and the dashed line shows the position of the virtual image. The focal lengths are represented by f_o and f_e.

Figure 2: Development of the telescope. (A) Positive objective lens. (B) Negative eyepiece lens. (C) Arrangement of lenses to ensure the focal lengths coincide at the correct point. The holder allows the lenses to be attached to a mount. (D) Unobstructed view of scene. (E) Scene viewed through the telescope, demonstrating magnification of the scene.

Mount on the mirror

The underlying refractive error of the participant was corrected, in order to optimise the magnification effect using MRI safe lenses. Corrective lenses fit underneath the telescope lens, and were in close proximity to both the eye and the telescopic lenses. Uncorrected refractive error would cause a reduction in the effective magnification and may lead to blurring of the target image. Under-correction of the refractive error would reduce the

effective power of the eyepiece lens, and therefore reduce the magnification achieved. Precise centration was essential to achieving adequate magnification and binocularity. The head mount was therefore designed to allow each lens to be moved in the X, Y and Z directions independently to provide fine tuning of centration for each eye (Figure 3).

The telescope mount was cut from acrylic glass tube, and the internal surface at each end turned down to provide keying points for the two lenses. Parallel grooves were cut into the outside walls of the tube allowing it to be griped between parallel rods. Translational movement along the rods accommodated for subject interocular distance.

The eyepiece lens was held in place by friction between the lens sides and the telescope tube wall, allowing for lens removal by applying pressure to the inner lens surface through the tube. The objective lens side wall had a circular groove cut to locate a small O-ring, allowing it to be held securely in the telescope tube while remaining easy to remove.

Acrylic glass was also used to create two side mounting plates for attachment to a commercially available head coil mirror (Figure 3A). A lateral slot in the mounting plate accommodated forward and backward movement along the scanner bore axis (Figure 3C).

Other components were fabricated from machinable plastic. A combination of keyed mounting blocks, and nylon screw-adjusted clutches supported the required independent axial movement. Mount design is available as CAD files https://github.com/jkjolly/Telescope_Mount.

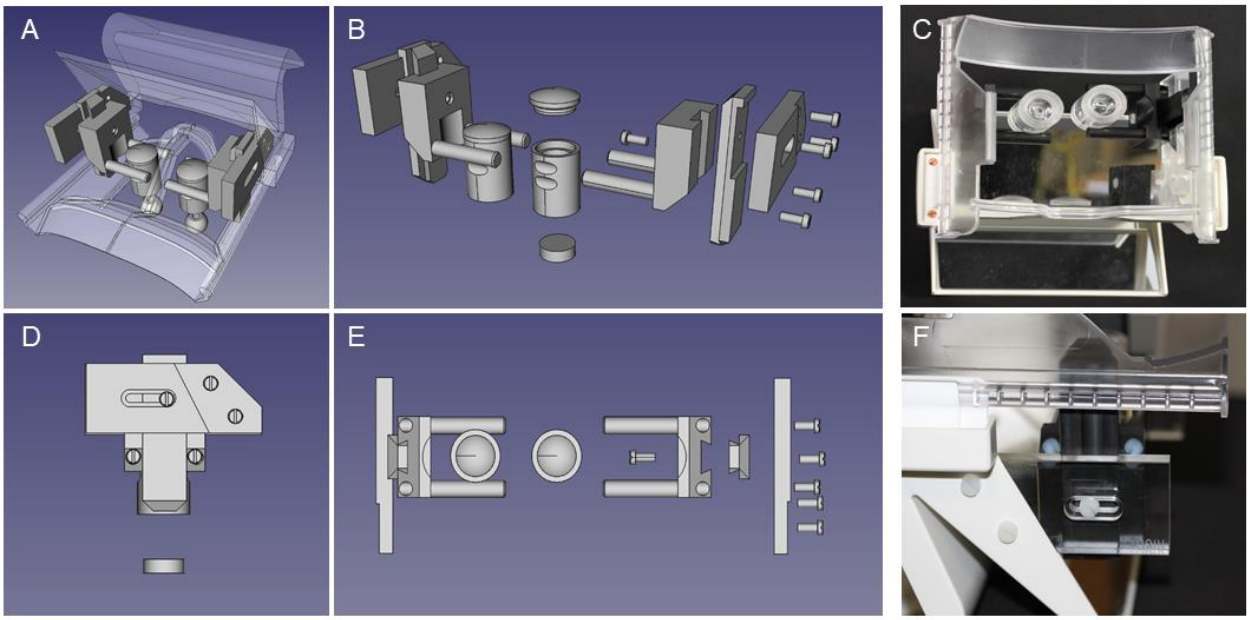

Figure 3: Mount assembly (A) Perspective view showing mounting location within mirror structure. (B) Exploded component perspective view showing component assembly. (C) Real world view from below. (D) Isometric side view showing assembled plates and screws. (E) Exploded components isometric view from below showing component assembly. (F) Real world side view.

Participants

Four healthy volunteers (three females/one male, aged 27 ± 5.4 (mean ± standard deviation, SD, years), participated in this study after giving informed consent. The experiment was performed under an agreed technical development protocol approved by the Oxford University Clinical Trials and Research Governance office, in accordance with International Electrotechnical Commission and United Kingdom Health Protection Agency guidelines. Subjects 1 and 2 had low levels of ametropia and were fully corrected. Subjects 3 and 4 had uncorrected astigmatism (≤ 1D), which was not possible to correct with the MRI safe glasses available at the time of scanning. In addition, subject 4 had high myopia (best vision sphere of -9D) and an intermittent exophoria which became manifest during scanning. The participants have a range of visual conditions as it is important to determine whether the presentation system is suitable for all.

Experimental Review

Visual stimulation with and without the telescope

Stimuli were generated in MATLAB (v 8.3, Mathworks Inc., Natick, MA, USA) using Psychtoolbox (v3.0, https://psychtoolbox.org) and displayed on an LCD display at the rear of the scanner bore (Brainard, 1997; Pelli, 1997). The participant viewed the display through correction glasses (if applicable), the telescope system, and a mirror mounted on the head coil.

The stimuli consisted of a radial checkerboard containing 48 black and white segments at 100% contrast, flickering in contrast at 2 Hz. The spatial frequencies increased from the centre to the periphery, using a base 10 log function, to account for eccentricity scaling within the visual cortex. The spatial frequency measured 4.35 cycles per degree (cpd) at the fovea and 1.18 cpd at the most eccentric point. Three different checkerboard sizes were used, of radial diameter 14.5° for large, 9.9° for medium and 5.7° for small. These were chosen arbitrarily as precise visual acuity is not important in assessment of the magnification effect on extent of stimulation. A red dot (0.5°) in the centre of the checkerboard was used for fixation. Stimuli were presented in a block design (block length of 15s), with each of the 3 different stimulus sizes, as well as a mid-grey blank screen, interleaved and presented 15 times. This produced a stimulation time of 900 seconds. Each participant performed two runs, one with the telescope and one without the telescope. Run order was counterbalanced across participants. The telescope doubled the field of view as a maximum to 29° for large, 19.8° for medium and 11.4° for small checkerboard.

MRI Acquisition

MR images were acquired with a 3T Prisma MRI scanner (Siemens Healthcare, Erlangen, Germany), using a 64-channel head coil. T1-weighted whole brain anatomical images were acquired with TR = 1900 ms, TE = 3.97 ms, TI = 904 ms, flip angle = 8°, slices = 192, resolution = 1mm isotropic. Functional images were acquired with a gradient echo EPI sequence TR = 1355ms, TE = 32.40 ms, flip angle = 70°, multiband factor 4, slices 72, 665 volumes and resolution = 2 mm isotropic. A B_0 field map was acquired to correct for

distortions due to field inhomogeneity TR= 482 ms, TE_1= 4.92 ms, TE_2 = 7.38 ms, resolution = 2 mm isotropic.

MRI Analysis

The fMRI scans were pre-processed using FEAT (FMRI Expert Analysis Tool) part of FSL (FMRIB Software Library V6 (Analysis Group, FMRIB, Oxford, UK; http://www.fmrib.ox.ac.uk/fsl)(Jenkinson, 2004, 2003; Woolrich et al., 2009). This involved motion correction using MCFLIRT (Jenkinson et al., 2002), brain extraction using BET (Smith, 2002), spatial smoothing using a Gaussian kernel (FWHM 4mm), grand-mean intensity normalisation of the entire 4D dataset by a single multiplicative factor, and highpass temporal filtering (Gaussian-weighted least-squares straight line fitting, with sigma=50.0s). One scan with motion artefacts was denoised using MELODIC (in FEAT) and FIX (Griffanti et al., 2014; Salimi-Khorshidi et al., 2014). Each fMRI run was spatially corrected for magnetic field inhomogeneities estimate by the B0 fieldmap and then registered to both the high resolution T1w structural scan and standard space using FLIRT (Jenkinson et al., 2002; Jenkinson and Smith, 2001).

Individual scan runs were analysed at the first level using FILM with local autocorrelation correction (Woolrich et al., 2001). Images were cluster-thresholded at $z > 3.1$, and clusters shown survived a statistical test for extent ($p < 0.05$, fully corrected for multiple comparisons) (Worlsey, 2001). At the high-level analysis stage, a paired t-test was computed across the group in order to compare activation with and without the telescope. Due to the small number of participants, a fixed effects model was used by forcing the random effects variance to zero in FLAME (FMRIB's Local Analysis of Mixed Effects)(Beckmann et al., 2003; Woolrich, 2008; Woolrich et al., 2004). Given the use of the fixed effects model, cluster-thresholding was applied at $z > 6.0$, and clusters survived a statistical test for extent ($p < 0.05$, fully corrected for multiple comparisons).

Results

<u>Visual stimulation through the telescope</u>

Once the eyepieces are correctly centred, the participant sees a single fused percept which is clear when fixation is central. The image fills the field of view up to the lens edge, with no obvious aberrations visible.

Visual cortex activity

As expected from a high contrast flickering checkerboard, there was extensive activation throughout the occipital pole across all conditions. Figure 4 shows the activation in each of the individual participants with and without the telescope-enabled expanded field of view for the largest stimulus. The activation is shown in both volume space and on a flattened cortical representation. Subjects 1-3 showed an increase in the volume of activated tissue using the telescope, evident both in the flattened, and volume view. This increase in activation is represented by the number of voxels activated in the primary visual cortex (V1) shown in Table 1. Interestingly, the increase in activated cortex is greater in the ventral side of the early visual cortex, particularly evident in the flattened representation. There is, however, some variability in the extent of increase, with Subject 1 showing the largest increase with the telescope. Due to the diplopia caused by the inability to fuse the images experienced by subject 4, this participant was excluded from the analysis. The presence of the diplopia would have caused suppression and hence a decrease in activation.

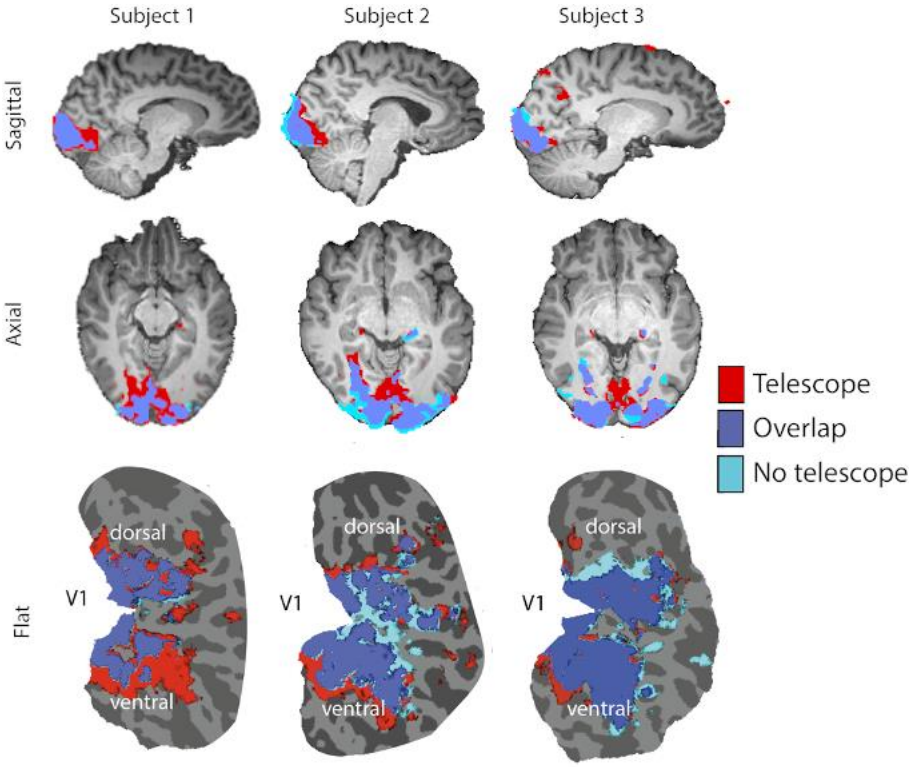

Figure 4: Cortical activation maps in response to the large stimulus size, both in volume space and on a flattened representation of the cortical surface. In each case, the red region reflects the neural response to the checkerboard stimulus with the telescope, cyan reflects activity without the telescope and purple is the overlap of the activation to the checkerboard with and without the telescope.

	Large		***Medium***		***Small***	
	Without Telescope	**With Telescope**	**Without Telescope**	**With Telescope**	**Without Telescope**	**With Telescope**
Subj01	1482	2152	1296	2141	648	1655
Subj02	1672	1794	1476	1765	1100	1259
Subj03	1405	1722	1052	1479	731	1075

Table 1: Number of voxels for each subject inside V1 that were activated with and without the telescope, for all stimulus conditions. V1 was defined by the Juelich histological atlas using FSL.(Amunts et al., 2000)

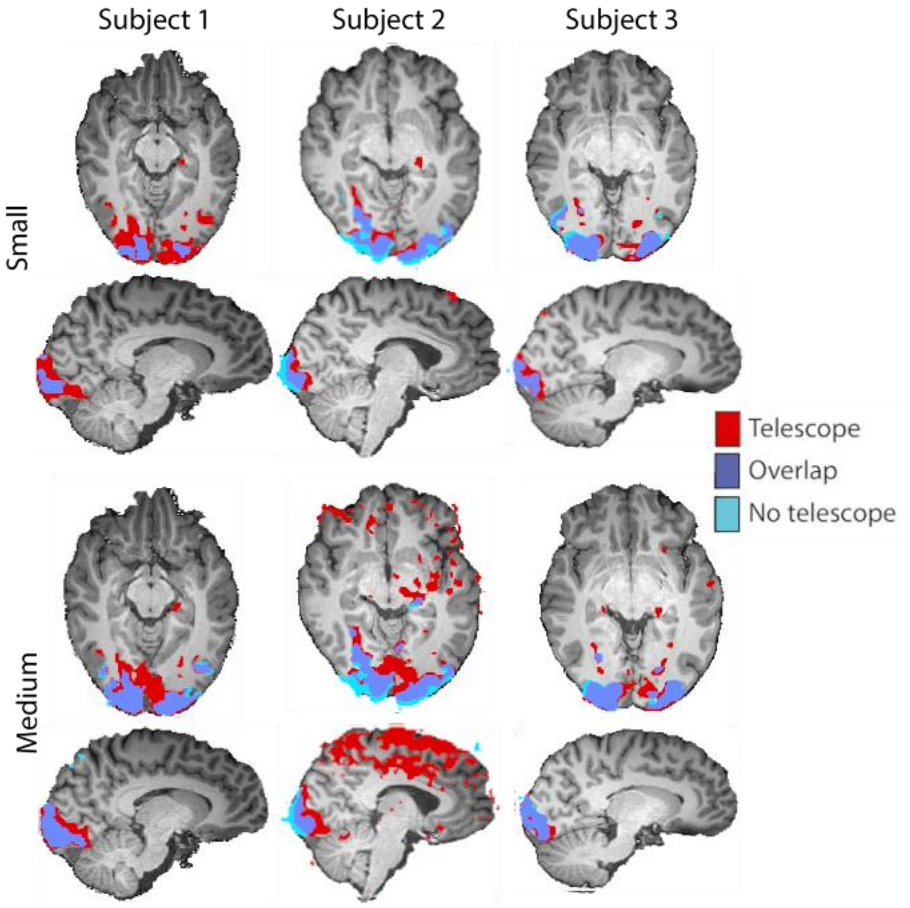

Figure 5: The activation generated by the small and medium stimulus sizes. As in Figure 4, the red reflects activity with the telescope, cyan activity reflects the response to the checkerboard without the telescope, and purple is the overlap of the activation to the checkerboard with and without the telescope.

Although most appropriate to investigate with the largest stimulus size, use of the telescope also increased the extent of activation when the smaller checkerboards were presented Figure 5). Again, there is considerable variability in the extent of increase in activation, with Subjects 1 and 2 showing a greater increase than Subject 3. However, in spite of the increased activity, Subject 2 shows evidence of head motion in response to the medium sized checkerboard, reflected in the artifactual activity along the midline. This is only present when using the telescope, suggesting that it might be related to fusion difficulties, although it is unclear why it is only present for the medium-sized stimulus.

A whole brain paired t-test comparing activation with the telescope compared to without the telescope shows the increased extent of activation across the calcarine sulcus at all three stimulus sizes in subjects 1-3 when the telescope is used (Figure 6). Note the anterior shift in the activity with increasing stimulus size.

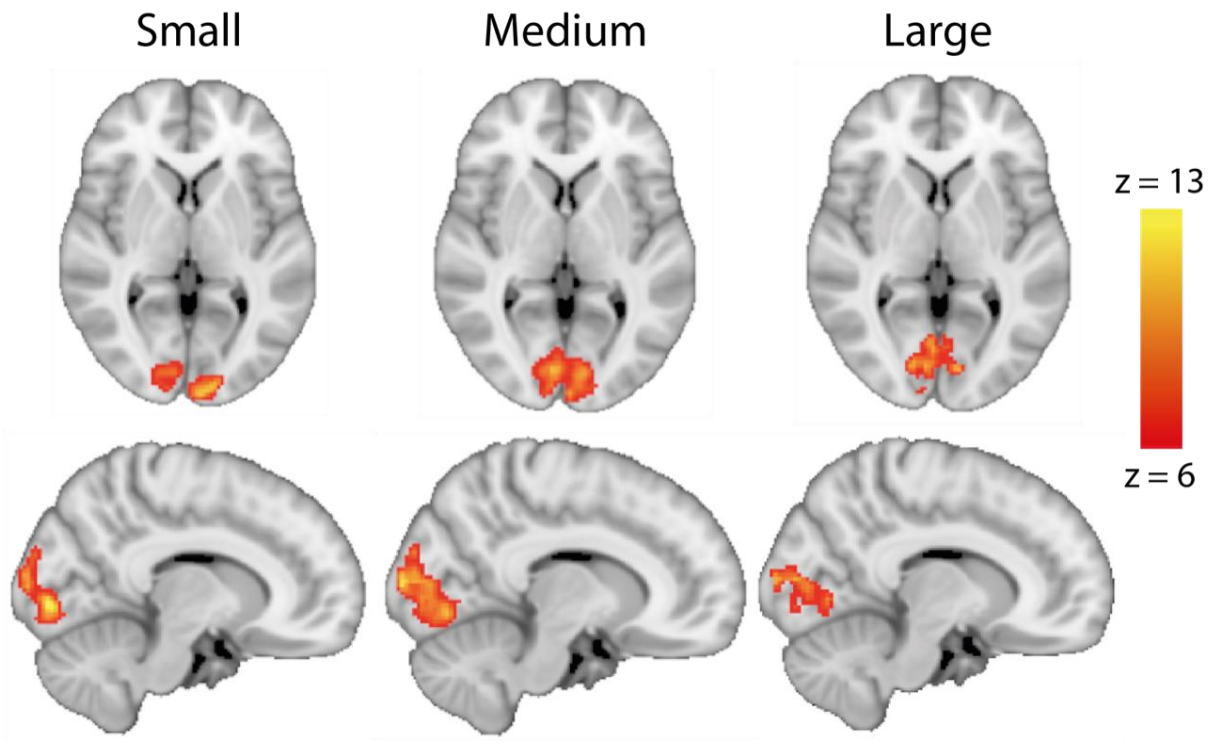

Figure 6: Regions of early visual cortex where stimulation viewed with the telescope evoked a greater response than no telescope, combined across the three participants with a fixed-effects analysis. Data are shown for the three stimulus sizes overlaid on the MNI152 brain.

Discussion

We demonstrate the use of a low-cost, MRI-compatible telescope that extends visual field coverage in a standard MRI environment. With adequate refractive correction, this system allows at least 2x magnification and therefore doubles the visual field visible within the scanner. When the lenses were fully aligned and the images fused, the overall BOLD activation was significantly greater with the telescope in place, reflecting the increased eccentricity of the activated cortical tissue.

We appreciate that using the same visual stimulation paradigm with and without the telescope leads to differences in the perceived stimulus, particularly regarding the spatial frequency of the checkerboard. There is, however, little evidence for the BOLD signal to be modulated by spatial frequency, either in terms of signal amplitude or extent (Swettenham et al., 2013).

The telescopic system is MR safe and can be easily implemented and removed with a standard MRI setup. It is a solution that is both low-cost and easy to manufacture. Commercially available lenses were ground and fitted into a custom-made mount that fits onto an existing MR mirror for ease of use. The lenses were individually fully manoeuvrable to optimise magnification achieved. Common perimetry techniques, such as the 10-2 grid implemented on several perimeters, covers the central 30 degrees of visual field. By expanding the field of view to a similar level, we allow the results from fMRI to be directly correlated with visual field testing due to the same area being covered.

While the telescope system has the potential to increase the visible visual field within the scanner, use of the system raises some practical issues. Firstly, while the basic attachment of the telescope is relatively straightforward, alignment of the images is challenging as it relies on participant feedback to detect fusion of the two images. Moreover, the lens alignment needs to be precise to achieve fusion, as without fusion the telescope system does not increase the visual field coverage. Since participant input is required to determine image fusion, patients with central vision loss are likely to have difficulty as they would not be able to foveate the stimuli. Patients with peripheral loss such as glaucoma or choroideremia who have spared central vision should, however, be able to fuse the images presented to the eyes. The telescope would provide a possible strategy to detect visual loss in these patient groups by increasing the visual field coverage into the periphery. Even participants who have healthy vision may have difficulty with image fusion due to refractive error, as in the case of subject 4. Correcting refractive error with goggles or contact lenses, however, should alleviate this issue, particularly if any astigmatism can also be corrected.

The Galilean telescope design was chosen for its practical implementation within the space available. For other scanners and head coils the system can be adapted by adjusting the lens powers and distances used. There are some known problems with the Galilean telescope designs such as vignetting, which reduces the brightness and clarity at borders (Katz, 2007). This is dependent on pupil size which varies from individual to individual. Along with chromatic aberration and other peripheral distortions, these would be larger with a larger

objective lens. The lens diameters were 25 mm, sufficiently small to reduce the impact of these factors. Additionally, the lenses were perfectly centred and the participant instructed to maintain central fixation, further reducing the impact of peripheral distortions. Finally, functional MRI analysis is not sensitive enough to determine low quality image versus a high quality image, or reduced visual acuity as shown earlier. The extent of the visual field receiving light input is the key metric.

A further practical limitation of the telescope system is the difficulty of integrating standard eye tracking. Eye tracking is commonly used in the MRI scanner to ensure that participants are maintaining fixation or making correct eye movements. Particularly when participants are required to perform a task at a specific retinal location, determining accurate location of the eyes is important. The majority of eye trackers require a 'line of sight' from the infra-red camera to the eye, often through use of the mirror used to view the stimuli. The presence of the telescope will impede the image of the eyes, and even when there is a line of sight, the lens system would create blurring of the ocular image that could not be corrected through the eye tracker focussing system.

In conclusion, the telescope system is a low-cost, MRI-compatible, easy to implement solution to increase the size of the effective visual field for fMRI experiments. While this system increases the extent of cortical activation due to the increased region of stimulation, it is likely to be most suitable for participants with healthy visual systems, who have prior experience in experiments. It may, however, also be useful to detect cortical changes in patients with loss of peripheral vision.

Acknowledgements

With thanks to Iain Wilson for his input into the original concept, Marcas O'Bardain for support in the workshop, and to the radiographers for their support in the testing of the telescope.

References

Amunts, K., Malikovic, A., Mohlberg, H., Schormann, T., Zilles, K., 2000. Brodmann's areas 17 and 18 brought into stereotaxic space - Where and how variable? Neuroimage 11,

66–84. https://doi.org/10.1006/nimg.1999.0516
Backus, B.T., Fleet, D.J., Parker, A.J., Heeger, D.J., 2001. Human cortical activity correlates with stereoscopic depth perception. J. Neurophysiol. 86, 2054–2068. https://doi.org/10.1152/jn.2001.86.4.2054
Baseler, H.A., Gouws, A., Haak, K. V., Racey, C., Crossland, M.D., Tufail, A., Rubin, G.S., Cornelissen, F.W., Morland, A.B., 2011. Large-scale remapping of visual cortex is absent in adult humans with macular degeneration. Nat. Neurosci. 14, 649–657. https://doi.org/10.1038/nn.2793
Beckmann, C.F., Jenkinson, M., Smith, S.M., 2003. General multilevel linear modeling for group analysis in FMRI. Neuroimage 20, 1052–1063. https://doi.org/10.1016/S1053-8119(03)00435-X
Brainard, D.H., 1997. The Psychophysics Toolbox. Spat. Vis. 10, 433–436. https://doi.org/10.1163/156856897X00357
Bridge, H., 2011. Mapping the visual brain: How and why. Eye 25, 291–296. https://doi.org/10.1038/eye.2010.166
Brown, H., Woodall, R.L., Kitching, R.E., Baseler, H.A., Morland, A.B., 2016. Using magnetic resonance imaging to assess visual deficits: a review. Ophthalmic Physiol. Opt. 36, 240–265. https://doi.org/10.1111/opo.12293
Choubey, B., Jurcoane, A., Muckli, L., Sireteanu, R., 2009. Methods for Dichoptic Stimulus Presentation in Functional Magnetic Resonance Imaging - A Review. Open Neuroimag. J. 3, 17–25. https://doi.org/10.2174/1874440000903010017
DeYoe, E.A., Carman, G.J., Bandettini, P., Glickman, S., Wieser, J., Cox, R., Miller, D., Neitz, J., 1996. Mapping striate and extrastriate visual areas in human cerebral cortex. Proc. Natl. Acad. Sci. 93, 2382–2386. https://doi.org/10.1073/pnas.93.6.2382
DeYoe, E.A., Ulmer, J.L., Mueller, W.M., Sabsevitz, D.S., Reitsma, D.C., Pillai, J.J., 2015. Imaging of the Functional and Dysfunctional Visual System. Semin. Ultrasound, CT MRI 36, 234–248. https://doi.org/10.1053/j.sult.2015.05.015
Dickinson, C., 2002. Low Vision Principles and Practice, Third edit. ed. Butterworth-Heinemann, Oxford.
Dumoulin, S.O., Knapen, T., 2018. How Visual Cortex Organization Is Altered by Ophthalmologic and Neurologic Disorders. Annu. Rev. Vis. Sci. 4, 7.1-7.23.
Dumoulin, S.O., Wandell, B.A., 2008. Population receptive field estimates in human visual cortex. Neuroimage 39, 647–660. https://doi.org/10.1016/j.neuroimage.2007.09.034
Griffanti, L., Salimi-khorshidi, G., Beckmann, C.F., Auerbach, J., Douaud, G., Sexton, C.E., Zsoldos, E., Ebmeier, K.P., Filippini, N., Mackay, C.E., Moeller, S., Xu, J., Yacoub, E., Baselli, G., Ugurbil, K., Miller, K.L., Smith, S.M., 2014. ICA-based artefact and accelerated fMRI acquisition for improved Resting State Network imaging. Neuroimage 95, 232–247. https://doi.org/10.1016/j.neuroimage.2014.03.034.ICA-based
Jenkinson, M., 2004. Improving the Registration of B0-disorted EPI Images using Calculated Cost Function Weights. Neuroimage 22, e1544–e1545.
Jenkinson, M., 2003. Fast, automated, N-dimensional phase-unwrapping algorithm. Magn. Reson. Med. 49, 193–197. https://doi.org/10.1002/mrm.10354
Jenkinson, M., Bannister, P., Brady, M., Smith, S., 2002. Improved optimization for the robust and accurate linear registration and motion correction of brain images. Neuroimage 17, 825–841. https://doi.org/10.1016/S1053-8119(02)91132-8
Jenkinson, M., Smith, S., 2001. A global optimisation method for robust affine registration of brain images. Med. Image Anal. 5, 143–156. https://doi.org/10.1016/S1361-8415(01)00036-6
Katz, M., 2007. Angular and Linear Fields of View of Galilean Telescopes and Telemicroscopes. Optom. Vis. Sci. 84, E522–E531.

373 https://doi.org/10.1097/OPX.0b013e31806db573
374 Neri, P., Bridge, H., Heeger, D.J., 2004. Stereoscopic processing of absolute and relative
375 disparity in human visual cortex. J. Neurophysiol. 92, 1880–1891.
376 https://doi.org/10.1152/jn.01042.2003
377 Pelli, D.G., 1997. The VideoToolbox software for visual psychophysics: transforming
378 numbers into movies. Spat. Vis. 10, 437–442.
379 Pitzalis, S., Sereno, M.I., Committeri, G., Fattori, P., Galati, G., Tosoni, A., Galletti, C.,
380 2013. The human homologue of macaque area V6A. Neuroimage 82, 517–530.
381 https://doi.org/10.1016/j.neuroimage.2013.06.026
382 Roby, J.W., Gao, J.H., Fox, P.T., 2000. A versatile, low-cost method for presenting visual
383 stimuli during MRI. J. Magn. Reson. Imaging 11, 223–227.
384 https://doi.org/10.1002/(SICI)1522-2586(200002)11:2<223::AID-JMRI22>3.0.CO;2-G
385 Salimi-Khorshidi, G., Douaud, G., Beckmann, C.F., Glasser, M.F., Griffanti, L., Smith, S.M.,
386 2014. Automatic denoising of functional MRI data: Combining independent component
387 analysis and hierarchical fusion of classifiers. Neuroimage 90, 449–468.
388 https://doi.org/10.1016/j.neuroimage.2013.11.046
389 Sereno, M.I., Dale, A.M., Reppas, J.B., Kwong, K.K., Belliveau, J.W., Brady, T.J., Rosen,
390 B.R., Tootell, R.B.., 1995. Borders of multiple visual areas in humans revealed by
391 functional MRI. Science (80-.). 268, 889–893.
392 Silson, E.H., Aleman, T.S., Willett, A., Serrano, L.W., Pearson, D.J., Rauschecker, A.M.,
393 Maguire, A.M., Baker, C.I., Bennett, J., Ashtari, M., 2018. Comparing clinical perimetry
394 and population receptive field measures in patients with choroideremia. Investig.
395 Ophthalmol. Vis. Sci. 59, 3249–3258. https://doi.org/10.1167/iovs.18-23929
396 Smith, S.M., 2002. Fast robust automated brain extraction. Hum. Brain Mapp. 17, 143–155.
397 https://doi.org/10.1002/hbm.10062
398 Swettenham, J.B., Muthukumaraswamy, S.D., Singh, K.D., 2013. BOLD responses in human
399 primary visual cortex are insensitive to substantial changes in neural activity. Front.
400 Hum. Neurosci. 7, 1–11. https://doi.org/10.3389/fnhum.2013.00076
401 Tootell, R.B.., Hadjikhani, N.K., Vanduffel, W., Liu, A.K., Mendola, J.D., Sereno, M.I.,
402 Dale, A.M., 1998. Functional analysis of primary visual cortex (V1) in humans. Proc.
403 Natl. Acad. Sci. 95, 811–817.
404 Wandell, B.A., Dumoulin, S.O., Brewer, A.A., 2007. Visual field maps in human cortex.
405 Neuron 56, 366–383. https://doi.org/10.1016/j.neuron.2007.10.012
406 Woolrich, M., 2008. Robust group analysis using outlier inference. Neuroimage 41, 286–301.
407 https://doi.org/10.1016/j.neuroimage.2008.02.042
408 Woolrich, M.W., Behrens, T.E.J., Beckmann, C.F., Jenkinson, M., Smith, S.M., 2004.
409 Multilevel linear modelling for FMRI group analysis using Bayesian inference.
410 Neuroimage 21, 1732–1747. https://doi.org/10.1016/j.neuroimage.2003.12.023
411 Woolrich, M.W., Jbabdi, S., Patenaude, B., Chappell, M., Makni, S., Behrens, T., Beckmann,
412 C., Jenkinson, M., Smith, S.M., 2009. Bayesian analysis of neuroimaging data in FSL.
413 Neuroimage 45, S173–S186. https://doi.org/10.1016/j.neuroimage.2008.10.055
414 Woolrich, M.W., Ripley, B.D., Brady, M., Smith, S.M., 2001. Temporal autocorrelation in
415 univariate linear modeling of FMRI data. Neuroimage 14, 1370–1386.
416 https://doi.org/10.1006/nimg.2001.0931
417 Worlsey, K.J., 2001. Statistical analysis of activation images, in: Jezzard, P., Matthews, P.M.,
418 Smith, S.M. (Eds.), Functional MRI: An Introduction to Methods. Oxford University
419 Press, Oxford, pp. 251–270.
420
421

Abstract

Background

A common limitation of typical projection systems used for visual fMRI is the limited field of view that can be presented to the observer within the scanner. A wide field of view over which stimuli can be presented is critical when investigating peripheral visual function, in particular visual disorders or diseases that lead to the loss of peripheral vision.

New method

We present a relatively low-cost Galilean telescopic device that can be used in most MRI scanners to double the effective visual field being presented. The system described is non-ferromagnetic, and compatible with most standard methods of visual presentation in MRI environments. The increase in area of visual cortex activation was quantified by comparing the extent of visual activity evoked by observing flickering checkerboards with and without the telescope in place.

Results

In all three observers that reported image fusion from the telescope, the extent of cortical activation was greater with the telescope, while in the fourth observer there was no difference between the two methods due to a lack of fusion.

Conclusion

The telescope is a low cost, easy to implement solution in situations where changes to the existing equipment or setup are not feasible.

Keywords: telescope; visual field; fMRI; visual cortex

Introduction

The early visual system is mapped in retinotopic coordinates, such that points that are adjacent to each other in the visual scene are represented by neighbouring neurons. This is the case from the photoreceptor cells in the retina through to the cerebral cortex, and provides the theoretical basis for retinotopic mapping; the identification of visual areas based on having one whole representation of visual space (Bridge, 2011; DeYoe et al., 1996; Sereno et al., 1995; Tootell et al., 1998).

Functional magnetic resonance imaging (fMRI) studies exploit retinotopy to identify different visual areas noninvasively. However, while the visual field of view is around 150° in natural vision, the limited space within the MRI environment significantly reduces the region visible from inside the scanner bore. Although the central visual field has considerably greater neural representation, known as cortical magnification (Wandell et al., 2007), there are many situations when peripheral stimulation is important (DeYoe et al., 2015). Firstly, in retinotopic mapping, the greater the stimulated region, the larger area of visual representation mapped in the cortex (Tootell et al., 1998). Secondly, some extrastriate visual areas, such as V6 and V6A primarily contain representations of the peripheral visual field, and cannot be accurately localised without far peripheral stimulation (Pitzalis et al., 2013). Thirdly, a lack of peripheral stimulation is a particular challenge when mapping the visual field in participants with eye disease that affects the periphery such as glaucoma, and rod-cone dystrophies (Brown et al., 2016; Silson et al., 2018). In the early stages of these conditions, vision loss can begin outside the area measurable by standard presentation methods. Therefore the cortical representation of this vision loss is not measured until the late stages of disease progression (Brown et al., 2016; Dumoulin and Knapen, 2018).

A number of different approaches are used to provide visual stimulation within the scanner environment, with one of the most common being a digital display placed at the end of the scanner bore. The screen is typically viewed using a standard mirror placed above the head of the scan participant, who lies supine on the scanner bed. This setup is limited by physical constraints, such as the scanner bore size, distance between the mirror and screen, and the physical apertures for the eyes provided in the head coil. A head-mounted goggle system can provide larger visual field coverage by using screens close to the eye (8,9). The main drawback of this type of system is the cost, which is significantly greater than other

presentation systems, and may not be suitable for participants with larger head sizes due to the space in the head coil. Another approach used to increase the stimulated field of view is a projector system with a target screen set close to the participant inside the scanner bore (Roby et al., 2000), but constraints on space make this option impossible for some scanning environments. Furthermore, errors can be induced by the close proximity of the screen to the eyes inducing convergence or accommodative errors. Solutions that require permanent installation of equipment are not feasible in scanner sites shared between multiple teams. The options available for presenting stimuli dichoptically have been previously comprehensively reviewed (Choubey et al., 2009), and include a system relying on Keplerian binoculars to separate the images to the two eyes (Neri et al., 2004).

In visual stimulation experiments using a screen outside the scanner bore, the stimulus typically extends up to around 13 degrees radius, though this varies on the specific setup in any particular center (Dumoulin and Wandell, 2008), with some set-ups reaching a maximum field of view with a radius up to 15 degrees (Baseler et al., 2011). Using a wide projection screen viewed directly without a mirror can increase the visual field up to 100 degrees (Pitzalis et al., 2013). However, this type of wide projection screen is difficult to set up due to the space requirements.

Telescopic systems allow the magnification of the stimulus, and therefore a greater area of the visual field to be covered by the stimulus. They can be attached directly to a standard MRI mirror, thus keeping the cost of the system low, and the time to implement short. Telescopes consist of two lenses set at specific distances from the eye and from each other in order to achieve optical magnification of the image. There are two telescopic designs that allow the creation of an image that is both magnified, and correctly oriented. Keplerian (or astronomical) telescopes as implemented in binoculars used previously (Backus et al., 2001; Neri et al., 2004) allow for greater levels of magnification but are generally large, and create an inverted image that must be rectified (albeit rectified by commercial binoculars). Nonetheless, the binoculars used previously relied on use of a surface coil on the occipital lobe, rather than the modern 64-channel head coils. Galilean telescopes are shorter and create a non-inverted image, therefore allowing for a more compact construction that is able to fit into the space available in the MRI environment between the eye and the head coil (Dickinson, 2002). The latter design was therefore chosen to fit in the limited space available

(Figure 1). The Galilean design is used in low vision devices such as the Eschenbach Max range which forms the inspiration for the design proposed.

Materials and Methods

Galilean telescope-based device

The principles of the design are shown in Figure 1. In our particular implementation, the objective lens had a power of +16.7D and the eyepiece lens had a power of -33D (Figure 2A and B). The lenses were placed 3cm apart so their focal lengths coincided, and the system was placed 3cm from the eye (Figure 2C). This resulted in 2x magnification as calculated by $M = -F_e / F_o$ (Figure 2D and E). In our test case using a 64-channel head coil (Siemens Healthcare, Erlangen, Germany) for a 3T Prisma MRI (Siemens Healthcare, Erlangen, Germany), the maximum space available between the MR safe glasses to the rim of the head coil was 3.6cm for both refractive correction and the telescopic system. This was a constraining factor for the lens powers that could be used. We also wanted to keep the objective lens as large as possible to maximise the field of view as the exit pupil diameter is equal to the objective lens diameter divided by the magnification. The lenses were crafted in polymethyl methacrylate with a refractive index of 1.4906 and no additional coating. They can be cut to size by any lab containing a lathe compatible with plastic lenses.

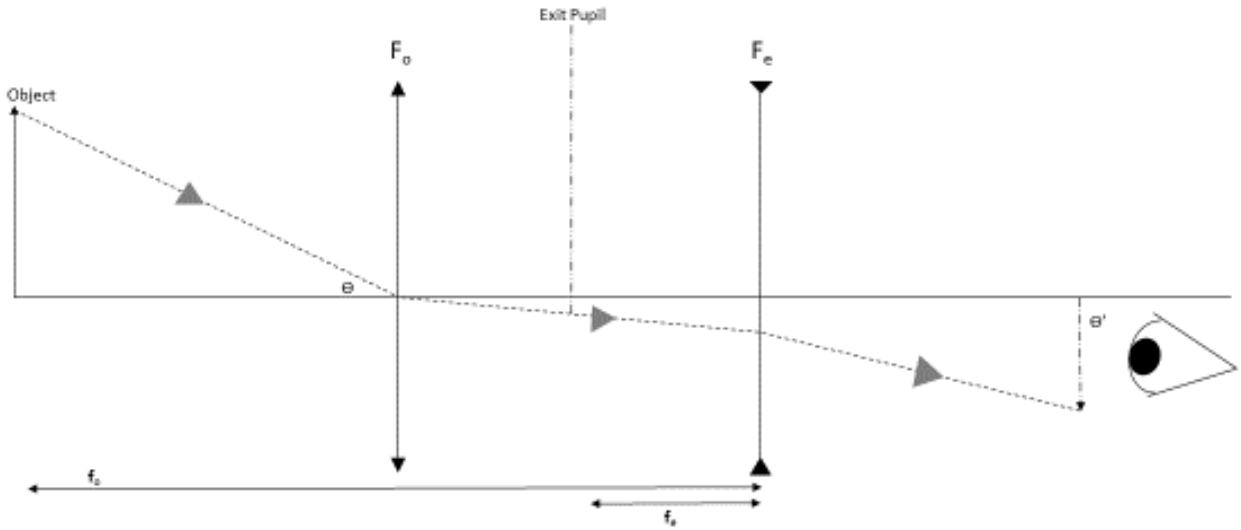

Figure 1: Ray diagram showing the principles of the Galilean telescope. The object extends angle Θ at the positive objective lens (F_o) and the image subtends angle Θ` at the eye. F_e denotes the negative eyepiece lens. The dotted line shows the path of light and the dashed line shows the position of the virtual image. The focal lengths are represented by f_o and f_e.

Figure 2: Development of the telescope. (A) Positive objective lens. (B) Negative eyepiece lens. (C) Arrangement of lenses to ensure the focal lengths coincide at the correct point. The holder allows the lenses to be attached to a mount. (D) Unobstructed view of scene. (E) Scene viewed through the telescope, demonstrating magnification of the scene.

Mount on the mirror

The underlying refractive error of the participant was corrected, in order to optimise the magnification effect using MRI safe lenses. Corrective lenses fit underneath the telescope lens, and were in close proximity to both the eye and the telescopic lenses. Uncorrected refractive error would cause a reduction in the effective magnification and may lead to blurring of the target image. Under-correction of the refractive error would reduce the

effective power of the eyepiece lens, and therefore reduce the magnification achieved. Precise centration was essential to achieving adequate magnification and binocularity. The head mount was therefore designed to allow each lens to be moved in the X, Y and Z directions independently to provide fine tuning of centration for each eye (Figure 3).

The telescope mount was cut from acrylic glass tube, and the internal surface at each end turned down to provide keying points for the two lenses. Parallel grooves were cut into the outside walls of the tube allowing it to be griped between parallel rods. Translational movement along the rods accommodated for subject interocular distance.

The eyepiece lens was held in place by friction between the lens sides and the telescope tube wall, allowing for lens removal by applying pressure to the inner lens surface through the tube. The objective lens side wall had a circular groove cut to locate a small O-ring, allowing it to be held securely in the telescope tube while remaining easy to remove.

Acrylic glass was also used to create two side mounting plates for attachment to a commercially available head coil mirror (Figure 3A). A lateral slot in the mounting plate accommodated forward and backward movement along the scanner bore axis (Figure 3C).

Other components were fabricated from machinable plastic. A combination of keyed mounting blocks, and nylon screw-adjusted clutches supported the required independent axial movement. Mount design is available as CAD files https://github.com/jkjolly/Telescope_Mount.

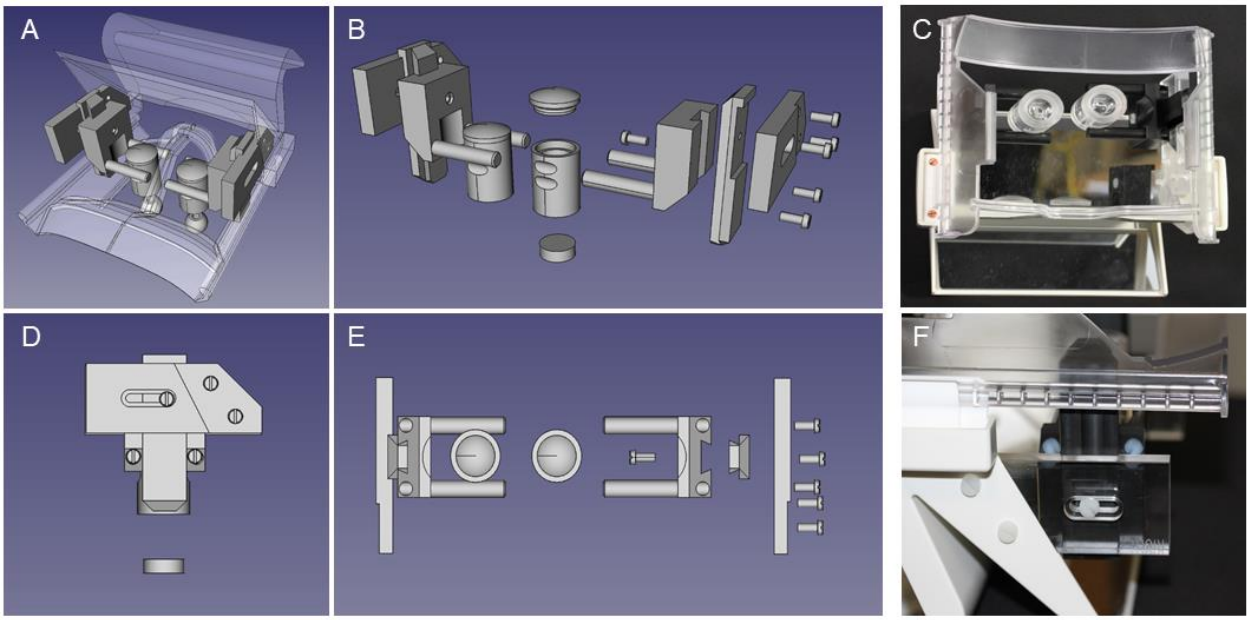

Figure 3: Mount assembly (A) Perspective view showing mounting location within mirror structure. (B) Exploded component perspective view showing component assembly. (C) Real world view from below. (D) Isometric side view showing assembled plates and screws. (E) Exploded components isometric view from below showing component assembly. (F) Real world side view.

Participants

Four healthy volunteers (three females/one male, aged 27 ± 5.4 (mean ± standard deviation, SD, years), participated in this study after giving informed consent. The experiment was performed under an agreed technical development protocol approved by the Oxford University Clinical Trials and Research Governance office, in accordance with International Electrotechnical Commission and United Kingdom Health Protection Agency guidelines. Subjects 1 and 2 had low levels of ametropia and were fully corrected. Subjects 3 and 4 had uncorrected astigmatism (≤ 1D), which was not possible to correct with the MRI safe glasses available at the time of scanning. In addition, subject 4 had high myopia (best vision sphere of -9D) and an intermittent exophoria which became manifest during scanning. The participants have a range of visual conditions as it is important to determine whether the presentation system is suitable for all.

Experimental Review

Visual stimulation with and without the telescope

Stimuli were generated in MATLAB (v 8.3, Mathworks Inc., Natick, MA, USA) using Psychtoolbox (v3.0, https://psychtoolbox.org) and displayed on an LCD display at the rear of the scanner bore (Brainard, 1997; Pelli, 1997). The participant viewed the display through correction glasses (if applicable), the telescope system, and a mirror mounted on the head coil.

The stimuli consisted of a radial checkerboard containing 48 black and white segments at 100% contrast, flickering in contrast at 2 Hz. The spatial frequencies increased from the centre to the periphery, using a base 10 log function, to account for eccentricity scaling within the visual cortex. The spatial frequency measured 4.35 cycles per degree (cpd) at the fovea and 1.18 cpd at the most eccentric point. Three different checkerboard sizes were used, of radial diameter 14.5° for large, 9.9° for medium and 5.7° for small. These were chosen arbitrarily as precise visual acuity is not important in assessment of the magnification effect on extent of stimulation. A red dot (0.5°) in the centre of the checkerboard was used for fixation. Stimuli were presented in a block design (block length of 15s), with each of the 3 different stimulus sizes, as well as a mid-grey blank screen, interleaved and presented 15 times. This produced a stimulation time of 900 seconds. Each participant performed two runs, one with the telescope and one without the telescope. Run order was counterbalanced across participants. The telescope doubled the field of view as a maximum to 29° for large, 19.8° for medium and 11.4° for small checkerboard.

MRI Acquisition

MR images were acquired with a 3T Prisma MRI scanner (Siemens Healthcare, Erlangen, Germany), using a 64-channel head coil. T1-weighted whole brain anatomical images were acquired with TR = 1900 ms, TE = 3.97 ms, TI = 904 ms, flip angle = 8°, slices = 192, resolution = 1mm isotropic. Functional images were acquired with a gradient echo EPI sequence TR = 1355ms, TE = 32.40 ms, flip angle = 70°, multiband factor 4, slices 72, 665 volumes and resolution = 2 mm isotropic. A B_0 field map was acquired to correct for

distortions due to field inhomogeneity TR= 482 ms, TE_1= 4.92 ms, TE_2 = 7.38 ms, resolution = 2 mm isotropic.

MRI Analysis

The fMRI scans were pre-processed using FEAT (FMRI Expert Analysis Tool) part of FSL (FMRIB Software Library V6 (Analysis Group, FMRIB, Oxford, UK; http://www.fmrib.ox.ac.uk/fsl)(Jenkinson, 2004, 2003; Woolrich et al., 2009). This involved motion correction using MCFLIRT (Jenkinson et al., 2002), brain extraction using BET (Smith, 2002), spatial smoothing using a Gaussian kernel (FWHM 4mm), grand-mean intensity normalisation of the entire 4D dataset by a single multiplicative factor, and highpass temporal filtering (Gaussian-weighted least-squares straight line fitting, with sigma=50.0s). One scan with motion artefacts was denoised using MELODIC (in FEAT) and FIX (Griffanti et al., 2014; Salimi-Khorshidi et al., 2014). Each fMRI run was spatially corrected for magnetic field inhomogeneities estimate by the B0 fieldmap and then registered to both the high resolution T1w structural scan and standard space using FLIRT (Jenkinson et al., 2002; Jenkinson and Smith, 2001).

Individual scan runs were analysed at the first level using FILM with local autocorrelation correction (Woolrich et al., 2001). Images were cluster-thresholded at $z > 3.1$, and clusters shown survived a statistical test for extent ($p < 0.05$, fully corrected for multiple comparisons) (Worlsey, 2001). At the high-level analysis stage, a paired t-test was computed across the group in order to compare activation with and without the telescope. Due to the small number of participants, a fixed effects model was used by forcing the random effects variance to zero in FLAME (FMRIB's Local Analysis of Mixed Effects)(Beckmann et al., 2003; Woolrich, 2008; Woolrich et al., 2004). Given the use of the fixed effects model, cluster-thresholding was applied at $z > 6.0$, and clusters survived a statistical test for extent ($p < 0.05$, fully corrected for multiple comparisons).

Results

<u>Visual stimulation through the telescope</u>

Once the eyepieces are correctly centred, the participant sees a single fused percept which is clear when fixation is central. The image fills the field of view up to the lens edge, with no obvious aberrations visible.

Visual cortex activity

As expected from a high contrast flickering checkerboard, there was extensive activation throughout the occipital pole across all conditions. Figure 4 shows the activation in each of the individual participants with and without the telescope-enabled expanded field of view for the largest stimulus. The activation is shown in both volume space and on a flattened cortical representation. Subjects 1-3 showed an increase in the volume of activated tissue using the telescope, evident both in the flattened, and volume view. This increase in activation is represented by the number of voxels activated in the primary visual cortex (V1) shown in Table 1. Interestingly, the increase in activated cortex is greater in the ventral side of the early visual cortex, particularly evident in the flattened representation. There is, however, some variability in the extent of increase, with Subject 1 showing the largest increase with the telescope. Due to the diplopia caused by the inability to fuse the images experienced by subject 4, this participant was excluded from the analysis. The presence of the diplopia would have caused suppression and hence a decrease in activation.

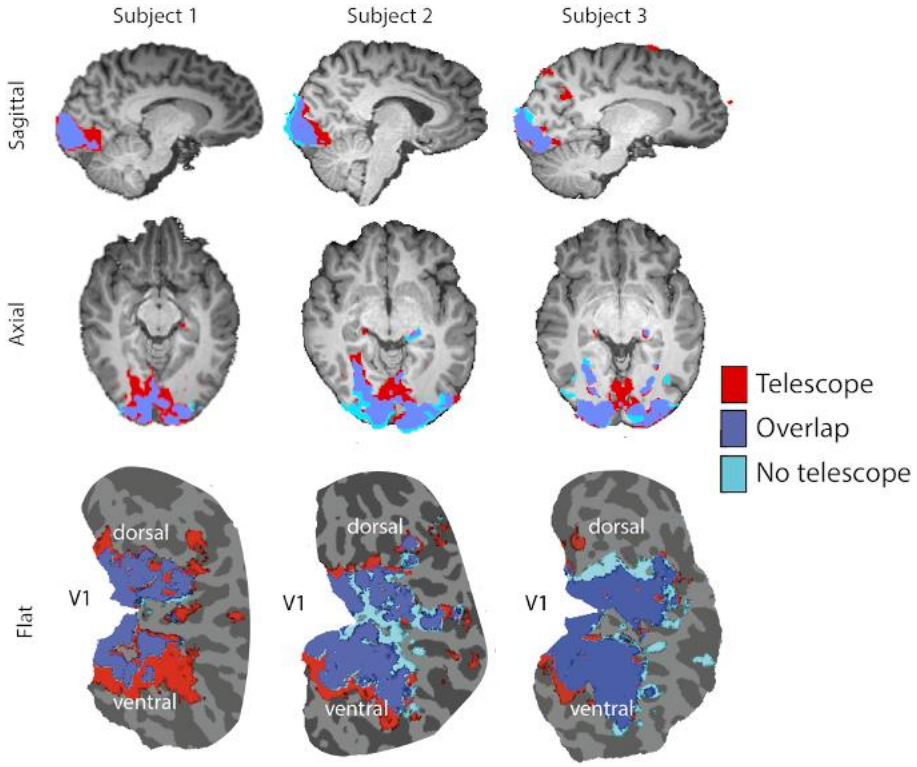

Figure 4: Cortical activation maps in response to the large stimulus size, both in volume space and on a flattened representation of the cortical surface. In each case, the red region reflects the neural response to the checkerboard stimulus with the telescope, cyan reflects activity without the telescope and purple is the overlap of the activation to the checkerboard with and without the telescope.

	Large		***Medium***		***Small***	
	Without Telescope	**With Telescope**	**Without Telescope**	**With Telescope**	**Without Telescope**	**With Telescope**
Subj01	1482	2152	1296	2141	648	1655
Subj02	1672	1794	1476	1765	1100	1259
Subj03	1405	1722	1052	1479	731	1075

Table 1: Number of voxels for each subject inside V1 that were activated with and without the telescope, for all stimulus conditions. V1 was defined by the Juelich histological atlas using FSL.(Amunts et al., 2000)

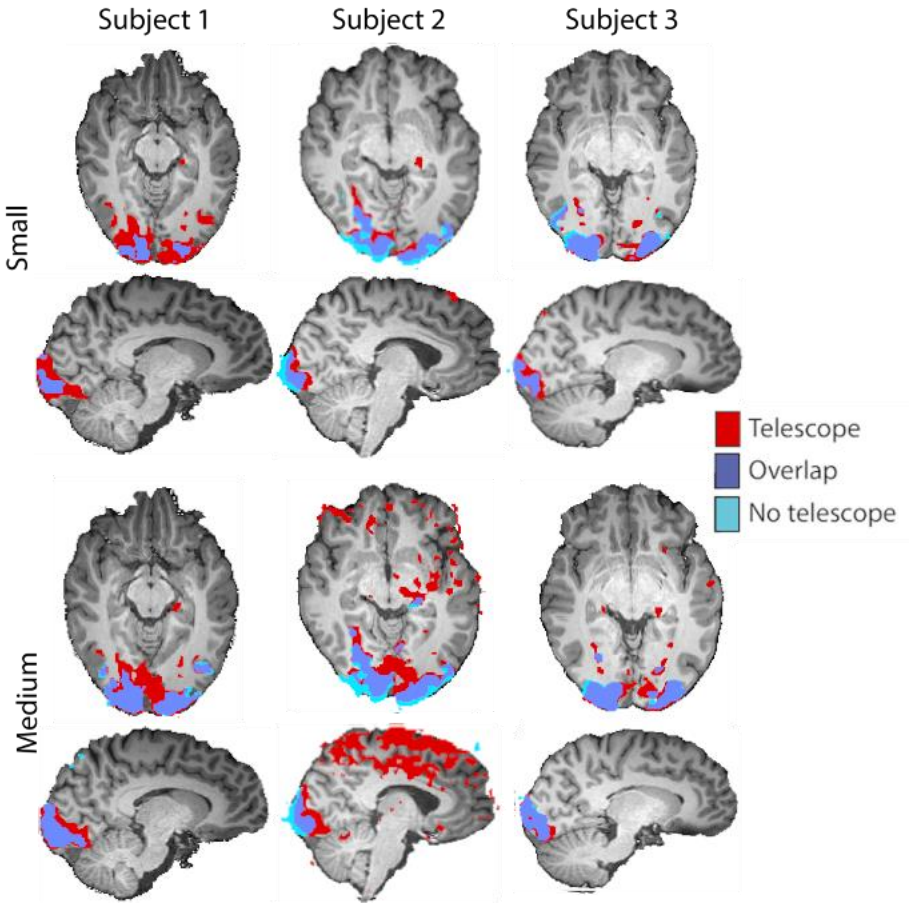

Figure 5: The activation generated by the small and medium stimulus sizes. As in Figure 4, the red reflects activity with the telescope, cyan activity reflects the response to the checkerboard without the telescope, and purple is the overlap of the activation to the checkerboard with and without the telescope.

Although most appropriate to investigate with the largest stimulus size, use of the telescope also increased the extent of activation when the smaller checkerboards were presented Figure 5). Again, there is considerable variability in the extent of increase in activation, with Subjects 1 and 2 showing a greater increase than Subject 3. However, in spite of the increased activity, Subject 2 shows evidence of head motion in response to the medium sized checkerboard, reflected in the artifactual activity along the midline. This is only present when using the telescope, suggesting that it might be related to fusion difficulties, although it is unclear why it is only present for the medium-sized stimulus.

A whole brain paired t-test comparing activation with the telescope compared to without the telescope shows the increased extent of activation across the calcarine sulcus at all three stimulus sizes in subjects 1-3 when the telescope is used (Figure 6). Note the anterior shift in the activity with increasing stimulus size.

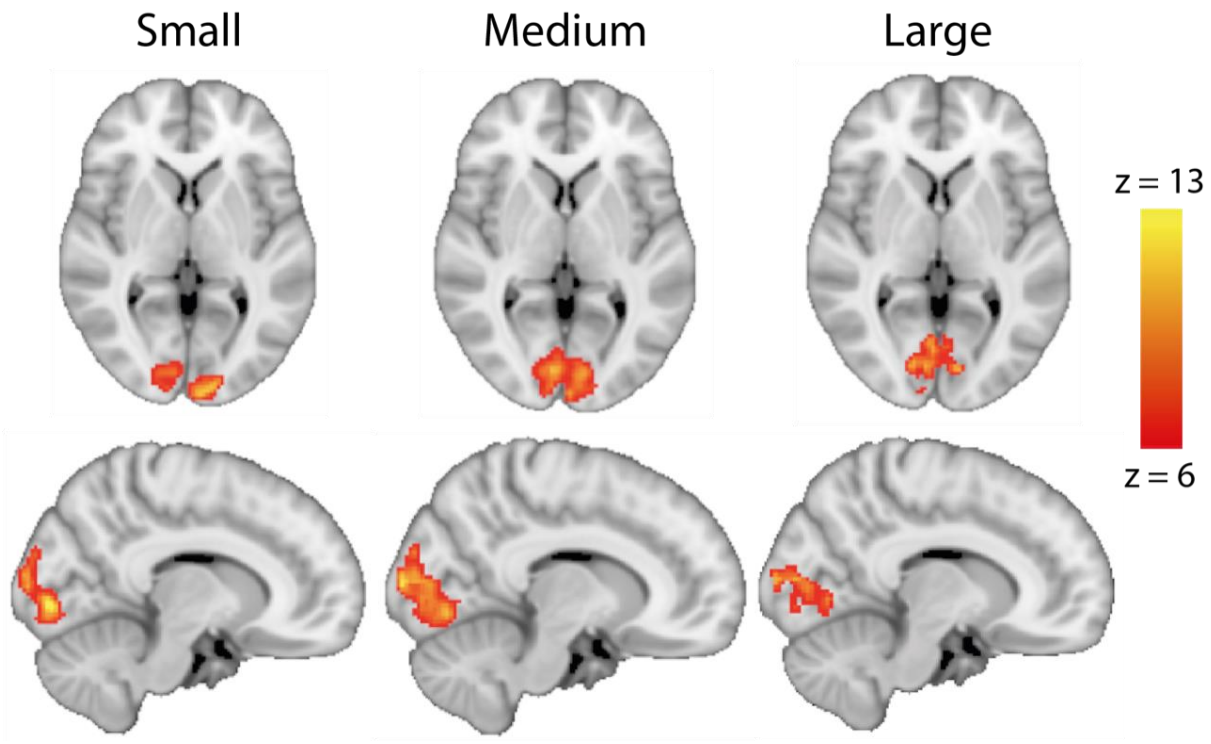

Figure 6: Regions of early visual cortex where stimulation viewed with the telescope evoked a greater response than no telescope, combined across the three participants with a fixed-effects analysis. Data are shown for the three stimulus sizes overlaid on the MNI152 brain.

Discussion

We demonstrate the use of a low-cost, MRI-compatible telescope that extends visual field coverage in a standard MRI environment. With adequate refractive correction, this system allows at least 2x magnification and therefore doubles the visual field visible within the scanner. When the lenses were fully aligned and the images fused, the overall BOLD activation was significantly greater with the telescope in place, reflecting the increased eccentricity of the activated cortical tissue.

We appreciate that using the same visual stimulation paradigm with and without the telescope leads to differences in the perceived stimulus, particularly regarding the spatial frequency of the checkerboard. There is, however, little evidence for the BOLD signal to be modulated by spatial frequency, either in terms of signal amplitude or extent (Swettenham et al., 2013).

The telescopic system is MR safe and can be easily implemented and removed with a standard MRI setup. It is a solution that is both low-cost and easy to manufacture. Commercially available lenses were ground and fitted into a custom-made mount that fits onto an existing MR mirror for ease of use. The lenses were individually fully manoeuvrable to optimise magnification achieved. Common perimetry techniques, such as the 10-2 grid implemented on several perimeters, covers the central 30 degrees of visual field. By expanding the field of view to a similar level, we allow the results from fMRI to be directly correlated with visual field testing due to the same area being covered.

While the telescope system has the potential to increase the visible visual field within the scanner, use of the system raises some practical issues. Firstly, while the basic attachment of the telescope is relatively straightforward, alignment of the images is challenging as it relies on participant feedback to detect fusion of the two images. Moreover, the lens alignment needs to be precise to achieve fusion, as without fusion the telescope system does not increase the visual field coverage. Since participant input is required to determine image fusion, patients with central vision loss are likely to have difficulty as they would not be able to foveate the stimuli. Patients with peripheral loss such as glaucoma or choroideremia who have spared central vision should, however, be able to fuse the images presented to the eyes. The telescope would provide a possible strategy to detect visual loss in these patient groups by increasing the visual field coverage into the periphery. Even participants who have healthy vision may have difficulty with image fusion due to refractive error, as in the case of subject 4. Correcting refractive error with goggles or contact lenses, however, should alleviate this issue, particularly if any astigmatism can also be corrected.

The Galilean telescope design was chosen for its practical implementation within the space available. For other scanners and head coils the system can be adapted by adjusting the lens powers and distances used. There are some known problems with the Galilean telescope designs such as vignetting, which reduces the brightness and clarity at borders (Katz, 2007). This is dependent on pupil size which varies from individual to individual. Along with chromatic aberration and other peripheral distortions, these would be larger with a larger

objective lens. The lens diameters were 25 mm, sufficiently small to reduce the impact of these factors. Additionally, the lenses were perfectly centred and the participant instructed to maintain central fixation, further reducing the impact of peripheral distortions. Finally, functional MRI analysis is not sensitive enough to determine low quality image versus a high quality image, or reduced visual acuity as shown earlier. The extent of the visual field receiving light input is the key metric.

A further practical limitation of the telescope system is the difficulty of integrating standard eye tracking. Eye tracking is commonly used in the MRI scanner to ensure that participants are maintaining fixation or making correct eye movements. Particularly when participants are required to perform a task at a specific retinal location, determining accurate location of the eyes is important. The majority of eye trackers require a 'line of sight' from the infra-red camera to the eye, often through use of the mirror used to view the stimuli. The presence of the telescope will impede the image of the eyes, and even when there is a line of sight, the lens system would create blurring of the ocular image that could not be corrected through the eye tracker focussing system.

In conclusion, the telescope system is a low-cost, MRI-compatible, easy to implement solution to increase the size of the effective visual field for fMRI experiments. While this system increases the extent of cortical activation due to the increased region of stimulation, it is likely to be most suitable for participants with healthy visual systems, who have prior experience in experiments. It may, however, also be useful to detect cortical changes in patients with loss of peripheral vision.

Acknowledgements

With thanks to Iain Wilson for his input into the original concept, Marcas O'Bardain for support in the workshop, and to the radiographers for their support in the testing of the telescope.

References

Amunts, K., Malikovic, A., Mohlberg, H., Schormann, T., Zilles, K., 2000. Brodmann's areas 17 and 18 brought into stereotaxic space - Where and how variable? Neuroimage 11,

66–84. https://doi.org/10.1006/nimg.1999.0516
Backus, B.T., Fleet, D.J., Parker, A.J., Heeger, D.J., 2001. Human cortical activity correlates with stereoscopic depth perception. J. Neurophysiol. 86, 2054–2068. https://doi.org/10.1152/jn.2001.86.4.2054
Baseler, H.A., Gouws, A., Haak, K. V., Racey, C., Crossland, M.D., Tufail, A., Rubin, G.S., Cornelissen, F.W., Morland, A.B., 2011. Large-scale remapping of visual cortex is absent in adult humans with macular degeneration. Nat. Neurosci. 14, 649–657. https://doi.org/10.1038/nn.2793
Beckmann, C.F., Jenkinson, M., Smith, S.M., 2003. General multilevel linear modeling for group analysis in FMRI. Neuroimage 20, 1052–1063. https://doi.org/10.1016/S1053-8119(03)00435-X
Brainard, D.H., 1997. The Psychophysics Toolbox. Spat. Vis. 10, 433–436. https://doi.org/10.1163/156856897X00357
Bridge, H., 2011. Mapping the visual brain: How and why. Eye 25, 291–296. https://doi.org/10.1038/eye.2010.166
Brown, H., Woodall, R.L., Kitching, R.E., Baseler, H.A., Morland, A.B., 2016. Using magnetic resonance imaging to assess visual deficits: a review. Ophthalmic Physiol. Opt. 36, 240–265. https://doi.org/10.1111/opo.12293
Choubey, B., Jurcoane, A., Muckli, L., Sireteanu, R., 2009. Methods for Dichoptic Stimulus Presentation in Functional Magnetic Resonance Imaging - A Review. Open Neuroimag. J. 3, 17–25. https://doi.org/10.2174/1874440000903010017
DeYoe, E.A., Carman, G.J., Bandettini, P., Glickman, S., Wieser, J., Cox, R., Miller, D., Neitz, J., 1996. Mapping striate and extrastriate visual areas in human cerebral cortex. Proc. Natl. Acad. Sci. 93, 2382–2386. https://doi.org/10.1073/pnas.93.6.2382
DeYoe, E.A., Ulmer, J.L., Mueller, W.M., Sabsevitz, D.S., Reitsma, D.C., Pillai, J.J., 2015. Imaging of the Functional and Dysfunctional Visual System. Semin. Ultrasound, CT MRI 36, 234–248. https://doi.org/10.1053/j.sult.2015.05.015
Dickinson, C., 2002. Low Vision Principles and Practice, Third edit. ed. Butterworth-Heinemann, Oxford.
Dumoulin, S.O., Knapen, T., 2018. How Visual Cortex Organization Is Altered by Ophthalmologic and Neurologic Disorders. Annu. Rev. Vis. Sci. 4, 7.1-7.23.
Dumoulin, S.O., Wandell, B.A., 2008. Population receptive field estimates in human visual cortex. Neuroimage 39, 647–660. https://doi.org/10.1016/j.neuroimage.2007.09.034
Griffanti, L., Salimi-khorshidi, G., Beckmann, C.F., Auerbach, J., Douaud, G., Sexton, C.E., Zsoldos, E., Ebmeier, K.P., Filippini, N., Mackay, C.E., Moeller, S., Xu, J., Yacoub, E., Baselli, G., Ugurbil, K., Miller, K.L., Smith, S.M., 2014. ICA-based artefact and accelerated fMRI acquisition for improved Resting State Network imaging. Neuroimage 95, 232–247. https://doi.org/10.1016/j.neuroimage.2014.03.034.ICA-based
Jenkinson, M., 2004. Improving the Registration of B0-disorted EPI Images using Calculated Cost Function Weights. Neuroimage 22, e1544–e1545.
Jenkinson, M., 2003. Fast, automated, N-dimensional phase-unwrapping algorithm. Magn. Reson. Med. 49, 193–197. https://doi.org/10.1002/mrm.10354
Jenkinson, M., Bannister, P., Brady, M., Smith, S., 2002. Improved optimization for the robust and accurate linear registration and motion correction of brain images. Neuroimage 17, 825–841. https://doi.org/10.1016/S1053-8119(02)91132-8
Jenkinson, M., Smith, S., 2001. A global optimisation method for robust affine registration of brain images. Med. Image Anal. 5, 143–156. https://doi.org/10.1016/S1361-8415(01)00036-6
Katz, M., 2007. Angular and Linear Fields of View of Galilean Telescopes and Telemicroscopes. Optom. Vis. Sci. 84, E522–E531.

373 https://doi.org/10.1097/OPX.0b013e31806db573
374 Neri, P., Bridge, H., Heeger, D.J., 2004. Stereoscopic processing of absolute and relative
375 disparity in human visual cortex. J. Neurophysiol. 92, 1880–1891.
376 https://doi.org/10.1152/jn.01042.2003
377 Pelli, D.G., 1997. The VideoToolbox software for visual psychophysics: transforming
378 numbers into movies. Spat. Vis. 10, 437–442.
379 Pitzalis, S., Sereno, M.I., Committeri, G., Fattori, P., Galati, G., Tosoni, A., Galletti, C.,
380 2013. The human homologue of macaque area V6A. Neuroimage 82, 517–530.
381 https://doi.org/10.1016/j.neuroimage.2013.06.026
382 Roby, J.W., Gao, J.H., Fox, P.T., 2000. A versatile, low-cost method for presenting visual
383 stimuli during MRI. J. Magn. Reson. Imaging 11, 223–227.
384 https://doi.org/10.1002/(SICI)1522-2586(200002)11:2<223::AID-JMRI22>3.0.CO;2-G
385 Salimi-Khorshidi, G., Douaud, G., Beckmann, C.F., Glasser, M.F., Griffanti, L., Smith, S.M.,
386 2014. Automatic denoising of functional MRI data: Combining independent component
387 analysis and hierarchical fusion of classifiers. Neuroimage 90, 449–468.
388 https://doi.org/10.1016/j.neuroimage.2013.11.046
389 Sereno, M.I., Dale, A.M., Reppas, J.B., Kwong, K.K., Belliveau, J.W., Brady, T.J., Rosen,
390 B.R., Tootell, R.B.., 1995. Borders of multiple visual areas in humans revealed by
391 functional MRI. Science (80-.). 268, 889–893.
392 Silson, E.H., Aleman, T.S., Willett, A., Serrano, L.W., Pearson, D.J., Rauschecker, A.M.,
393 Maguire, A.M., Baker, C.I., Bennett, J., Ashtari, M., 2018. Comparing clinical perimetry
394 and population receptive field measures in patients with choroideremia. Investig.
395 Ophthalmol. Vis. Sci. 59, 3249–3258. https://doi.org/10.1167/iovs.18-23929
396 Smith, S.M., 2002. Fast robust automated brain extraction. Hum. Brain Mapp. 17, 143–155.
397 https://doi.org/10.1002/hbm.10062
398 Swettenham, J.B., Muthukumaraswamy, S.D., Singh, K.D., 2013. BOLD responses in human
399 primary visual cortex are insensitive to substantial changes in neural activity. Front.
400 Hum. Neurosci. 7, 1–11. https://doi.org/10.3389/fnhum.2013.00076
401 Tootell, R.B.., Hadjikhani, N.K., Vanduffel, W., Liu, A.K., Mendola, J.D., Sereno, M.I.,
402 Dale, A.M., 1998. Functional analysis of primary visual cortex (V1) in humans. Proc.
403 Natl. Acad. Sci. 95, 811–817.
404 Wandell, B.A., Dumoulin, S.O., Brewer, A.A., 2007. Visual field maps in human cortex.
405 Neuron 56, 366–383. https://doi.org/10.1016/j.neuron.2007.10.012
406 Woolrich, M., 2008. Robust group analysis using outlier inference. Neuroimage 41, 286–301.
407 https://doi.org/10.1016/j.neuroimage.2008.02.042
408 Woolrich, M.W., Behrens, T.E.J., Beckmann, C.F., Jenkinson, M., Smith, S.M., 2004.
409 Multilevel linear modelling for FMRI group analysis using Bayesian inference.
410 Neuroimage 21, 1732–1747. https://doi.org/10.1016/j.neuroimage.2003.12.023
411 Woolrich, M.W., Jbabdi, S., Patenaude, B., Chappell, M., Makni, S., Behrens, T., Beckmann,
412 C., Jenkinson, M., Smith, S.M., 2009. Bayesian analysis of neuroimaging data in FSL.
413 Neuroimage 45, S173–S186. https://doi.org/10.1016/j.neuroimage.2008.10.055
414 Woolrich, M.W., Ripley, B.D., Brady, M., Smith, S.M., 2001. Temporal autocorrelation in
415 univariate linear modeling of FMRI data. Neuroimage 14, 1370–1386.
416 https://doi.org/10.1006/nimg.2001.0931
417 Worlsey, K.J., 2001. Statistical analysis of activation images, in: Jezzard, P., Matthews, P.M.,
418 Smith, S.M. (Eds.), Functional MRI: An Introduction to Methods. Oxford University
419 Press, Oxford, pp. 251–270.
420
421

CRediT author statement

Jasleen K Jolly: Conceptualization, methodology, validation, investigation, writing-original draf, visualization, project administration

Aislin Sheldon: Software, validation, formal analysis, investigation, writing-review & editing, visualization

Ivan Alvarez: Software, investigation, writing-review & editing

Chris Gallagher: Software, data curation, writing-review & editing, visualization

Robert E MacLaren: Resources, writing-review & editing, supervision

Holly Bridge: Methodology, validation, formal analysis, resources, writing-review & editing, supervision

The authors report no conflict of interest.